Thermodynamics of high-T_C materials in the rotating antiferromagnetism theory

Mohamed Azzouz
Department of Physics and Astronomy, Laurentian University, Ramsey Lake Road, Sudbury, Ontario, Canada P3E 2C6
(Received 20 June 2003; published 21 November 2003)

In high-temperature superconductors the pseudogap energy affects the electronic specific-heat data for doping densities smaller than the optimal point. Within the rotating antiferromagnetism theory I calculated the superconducting and rotating antiferromagnetic parameters, then got the phase diagram. Also, the specific-heat coefficient and entropy are evaluated as a function of temperature. In addition, the doping dependence of the condensation energy, specific-heat anomaly, and entropy at T_C are calculated. Experimental data are analyzed by focusing on the trends in the doping and temperature dependence. As far as the above quantities are concerned this theory yields very good agreement with experiment, and can therefore be said to be applicable to high-temperature superconductors.

DOI: 10.1103/PhysRevB.68.174523 PACS number(s): 74.25.Bt, 74.25.Ha

I. INTRODUCTION

The rotating antiferromagnetism theory (RAFT) I have recently proposed[1] addresses the issue of the pseudogap (PG) phenomenon[2] and the doping dependence of the electronic structure in high-temperature superconductors[3] (HTSC's). RAFT is based on spin antiferromagnetism (AF) and is therefore fundamentally different from the density *d*-wave (DDW) theory[4] which is based on orbital AF. Furthermore, rotational symmetry is not broken in RAFT because the rotating order parameter characterizing rotating antiferromagnetism (RAF) is a magnetization that has a finite average magnitude but a random phase angle. Also, very recently I proposed to treat the CuO_2 layers of HTSC's as open systems in contact with a particle reservoir, which is formed by the atoms doped between these layers. To leading order, one can model the low-energy physics of HTSC's by considering a two-dimensional (2D) lattice of electrons in contact with a thermodynamics electrons reservoir. As a consequence, the charge-carrier density on the CuO_2 layers is temperature dependent.[5] This T dependence should not be surprising in the light of the strong T dependence of the Hall coefficient.[6–8] In the present work I tested the applicability of RAFT and the above ideas at finite temperature by calculating several thermodynamic functions and comparing them with their experimental data. I calculated the temperature dependence of RAFT's order parameters, the electronic entropy $S_{el}(T)$ and the specific-heat $C_{el}(T)$ or coefficient $\gamma(T)=C_{el}(T)/T$. I also investigated the doping dependence of the condensation energy U_0, the entropy at T_C, $S(T_C)$, and the jump in $\gamma(T)$ at the superconducting transition temperature T_C.

One of the important questions that I also addressed in this work is whether there exists a true phase transition below which the PG appears or not. Experimentally, no specific-heat anomaly due to the PG has been reported so far. In this paper, I propose two possible scenarios to explain the absence of experimental evidence for such an anomaly. In the first scenario, the anomaly in $\gamma(T)$ due to the PG goes unnoticed because it is significantly smaller than the one due to superconductivity (SC) especially in the neighborhood of the optimal point. In the second scenario, the PG temperature T^* stays much higher than the superconducting transition temperature T_C as doping increases away form half filling even though the PG *order parameter* itself is significantly reduced and vanishes near the optimal point. According to both scenarios, to observe the anomaly at T^* one should not be looking for a λ-shape (or peak) anomaly but rather for a steplike one in the specific-heat coefficient. In the second scenario, this anomaly occurs at temperatures much higher than T_C even near optimal doping. Furthermore, I show that RAFT yields specific-heat results that are consistent with the conclusion of Loram and co-workers.[9] These authors concluded that the simplest interpretation of the specific-heat data can be done in terms of carriers that are fermions with a very low Fermi temperature, which is of the order of 10^3 K. RAFT has been found to agree well with ground-state experimental data when I indeed assumed that the electronic hopping energies are small.[1]

This paper is organized as follows. In Sec. II, RAFT is briefly reviewed, and the idea of the CuO_2 layers behaving as open systems is explained. For the results presented in this paper, two Hamiltonian parameters sets are used to carry on the numerical calculations. The analysis of the temperature dependence of the rotating and superconducting order parameters is presented in Sec. III. In the latter, the temperature dependence of doping is analyzed as well, and used to discuss the T dependence of the Hall coefficient in HTSC's. Furthermore, I focus on the doping dependence of the superconducting transition temperature T_C and PG temperature T^* in Sec. IV, where the phase diagrams are calculated for both Hamiltonian parameters sets. The specific-heat coefficient and entropy results are presented in Sec. V. The doping dependence of superfluidity is studied in Sec. VI. Finally, the summary and conclusions are given in Sec. VII.

II. DESCRIPTION OF THE METHOD

RAFT is a theory that describes HTSC's in terms of two competing order parameters. One of these is proportional to the superconducting gap amplitude, and is called D_0, and the second one is the RAF parameter labeled Q. The latter is the amplitude of a rotating magnetization, which I have proposed in order to model the PG behavior in the cuprates.

RAFT is based on the rotating order parameter concept[10] first applied to the Kondo lattice model. This concept has been generalized to the case of HTSC's for which several ground-state properties have been calculated and successfully compared with experiment.[1] The rotating staggered magnetization Q is related to the spin raising or lowering operator, and is thus a measure of the spin quantum fluctuations. RAFT proposes that below the so-called PG temperature the spin quantum fluctuations give rise to some sort of *hidden order* with order parameter Q, which does not break rotational symmetry. It is not yet really clear to me what precise experiment would probe this hidden order. Perhaps, an external rotating magnetic field and a static magnetic field perpendicular to each other would favor the rotating magnetization on one sublattice over the other. This would give rise to a signal that could be measurable. As for the spin-glass phase of HTSC's, I do not see yet any link between the rotating magnetization Q and the spin-glass state. Claiming it is possible that the rotating order may give rise to spin-glass order as the rotating staggered magnetization freezes at low temperature would be pure speculation, presently. For convenience, I will now briefly review this theory in Sec. II A, and explain the idea of CuO_2 layers being open systems in Sec. II B. This idea leads to a T dependent charge-carrier density.

A. Review of RAFT

The Hamiltonian considered in this study is the extended Hubbard model with a repulsive on-site Coulomb interaction U and an effective nearest-neighbor attractive interaction V.[11] It reads as follows:

$$H=-\sum_{i,j,\sigma} t_{ij}c^{\dagger}_{i,\sigma}c_{j,\sigma}-\mu\sum_{i,\sigma} c^{\dagger}_{i,\sigma}c_{i,\sigma}+U\sum_{i} n_{i,\uparrow}n_{i,\downarrow} -V\sum_{\langle i,j\rangle} n_{i,\uparrow}n_{j,\downarrow}, \tag{1}$$

where t_{ij} designates electronic hopping amplitudes to first, second, third, and fourth nearest neighbors t, t', t'', and t''', respectively, on a 2D square lattice. μ is the chemical potential. At the mean-field level, the eight vector

$$\mathcal{C}^{\dagger}_{\mathbf{k}}=(c^{A}_{-\mathbf{k}\uparrow}{}^{\dagger},c^{B}_{-\mathbf{k}\uparrow}{}^{\dagger},c^{A}_{\mathbf{k}\downarrow},c^{B}_{\mathbf{k}\downarrow},c^{A}_{\mathbf{k}\uparrow},c^{B}_{\mathbf{k}\uparrow},c^{A}_{-\mathbf{k}\downarrow}{}^{\dagger},c^{B}_{-\mathbf{k}\downarrow}{}^{\dagger}) \tag{2}$$

is used in order to cast the Hamiltonian into the bilinear form

$$H_{MS}=\sum_{\mathbf{k}_<} \mathcal{C}^{\dagger}_{\mathbf{k}}\mathcal{H}\mathcal{C}_{\mathbf{k}}+NUQ^2+4NVD_0^2-NUn^2-\sum_{\mathbf{k}} \mu'(\mathbf{k}), \tag{3}$$

where $\mathcal{H}$ is an 8×8 matrix,

$$\mathcal{H}=\begin{pmatrix} \mathcal{H}' & \mathcal{U}_Q \\ -\mathcal{U}_Q & -\mathcal{H}' \end{pmatrix},$$

with $\mathcal{H}'$ and $\mathcal{U}_Q$, two 4×4 matrices, given, respectively, by

$$\mathcal{H}'=\begin{pmatrix} -\mu'(\mathbf{k}) & \epsilon(\mathbf{k}) & 0 & D(\mathbf{k}) \\ \epsilon(\mathbf{k}) & -\mu'(\mathbf{k}) & D(\mathbf{k}) & 0 \\ 0 & D(\mathbf{k}) & \mu'(\mathbf{k}) & -\epsilon(\mathbf{k}) \\ D(\mathbf{k}) & 0 & -\epsilon(\mathbf{k}) & \mu'(\mathbf{k}) \end{pmatrix}$$

and

$$\mathcal{U}_Q=\begin{pmatrix} 0 & 0 & QU & 0 \\ 0 & 0 & 0 & -QU \\ -QU & 0 & 0 & 0 \\ 0 & QU & 0 & 0 \end{pmatrix}.$$

The effective chemical potential $\mu'(\mathbf{k})$ is given by

$$\mu'(\mathbf{k})=\mu-Un+4t'\cos k_x\cos k_y+2t''[\cos(2k_x)+\cos(2k_y)], \tag{4}$$

and $n=\langle c^{\dagger}_{i,\sigma}c_{i,\sigma}\rangle$ is the electron density per site and spin; $\sigma=\uparrow$ or $\downarrow$. The summation symbol $\Sigma_{\mathbf{k}_<}$ takes into account the fact that I sum over $\mathbf{k}$ and its opposite, and also over the two antiferromagnetic sublattices A and B. The free energy per site is given by

$$F=-\frac{1}{2N\beta}\sum_{\mathbf{k}}\sum_{\eta=\pm,\nu=1,2}\ln\{1+e^{-\eta\beta E_{\nu}(\mathbf{k})}\}+4VD_0^2+UQ^2 -Un^2-\frac{1}{N}\sum_{\mathbf{k}} \mu'(\mathbf{k}). \tag{5}$$

Here, N is the total number of lattice sites, and the energy spectra are given by $\pm E_1(\mathbf{k})$ and $\pm E_2(\mathbf{k})$ with

$$E_{\nu}(\mathbf{k})=\sqrt{[\mu'(\mathbf{k})+(-1)^{\nu}E_q(\mathbf{k})]^2+D^2(\mathbf{k})}, \tag{6}$$

where $\nu=1$ or 2, $D(\mathbf{k})=2VD_0(\cos k_x-\cos k_y)$, $E_q(\mathbf{k})=\sqrt{\epsilon^2(\mathbf{k})+Q^2U^2}$, $\epsilon(\mathbf{k})=-2t(\cos k_x+\cos k_y)-4t'''[\cos(kx)\cos(2k_y)+\cos(k_y)\cos(2k_x)]$, and $\beta=1/k_BT$; k_B being the Boltzmann constant. Upon minimizing the free energy F with respect to $Q=|\langle c_{i,\uparrow}c^{\dagger}_{i,\downarrow}\rangle|$ and $D_0=|\langle c_{i,\uparrow}c_{j,\downarrow}\rangle|$, with i and j labeling adjacent sites, I derived the following mean-field equations:

$$1=\frac{V}{4N}\sum_{\mathbf{k},\nu=1,2}\frac{(\cos k_x-\cos k_y)^2}{E_{\nu}}\tanh\left(\frac{\beta E_{\nu}}{2}\right),$$

$$1=\frac{U}{4N}\sum_{\mathbf{k},\nu=1,2}(-1)^{\nu+1}\frac{A_{\nu}}{E_q}\tanh\left(\frac{\beta E_{\nu}}{2}\right),$$

$$n=-\frac{1}{4N}\sum_{\mathbf{k},\nu=1,2}A_{\nu}\tanh\left(\frac{\beta E_{\nu}}{2}\right)+\frac{1}{2}, \tag{7}$$

where

$$A_{\nu}(\mathbf{k})=[-\mu'(\mathbf{k})-(-1)^{\nu}E_q(\mathbf{k})]/E_{\nu}(\mathbf{k}). \tag{8}$$

Note that contrary to Ref. 1 where only electrons hopping to as far as second nearest neighbors were taken into account,

TABLE I. The two sets of the Hamiltonian parameters used in this paper to carry on the numerical calculations are summarized in this table. The unit of energy is $t=1$.

	U	V	t'	t''	t'''
SET I	$3t$	t	$-0.25t$	0	0
SET II	$2.8t$	$0.85t$	$-0.16t$	$0.01t$	$-0.05t$

hopping energies up to fourth nearest neighbors have been considered in the present study. This is necessary in order to adjust the location of the superconducting dome in the calculated phase diagram to fit better the experimental phase diagram. Notice the peculiar way these terms appear in the effective chemical potential $\mu'(\mathbf{k})$ and in the single-electron energy $\epsilon(\mathbf{k})$. Hopping terms connecting different sublattices appear in $\epsilon(\mathbf{k})$, whereas those connecting same sublattices appear in $\mu'(\mathbf{k})$.

B. Hypothesis for solving the mean-field equations

The low-energy physical properties of HTSC's are believed to be governed by the motion of electrons within the copper-oxide layers. This is why 2D Hubbard-type models are utilized so often for the study of these materials. Recently (Ref. 5), I proposed that the atoms doped between the CuO_2 layers constitute a charge reservoir with the number of electrons much greater than the number of electrons on CuO_2 layers. The chemical potential μ is therefore fixed by these interlayer reservoirs. To leading order in the thermodynamics treatment of these reservoirs (where they are considered thermodynamic particle reservoirs), μ can be taken to be temperature independent. As a consequence of this hypothesis, to solve Eqs. (7) I fix the chemical potential and calculate the density n as a function of T. In this way both the electron and hole densities $2n$ and $p=1-2n$, respectively, are T dependent. Normally, for a closed system, such as a gas of electrons in a conventional metal, no temperature dependence is shown by the density of electrons. The procedure that is followed in that case consists of fixing the density and solving for the chemical potential as a function of temperature. One of the interesting implications of this hypothesis is the explanation of the T dependence of the Hall coefficient.[5]

III. THE ROTATING AND SUPERCONDUCTING ORDER PARAMETERS Q AND D_0

A. The doping dependence of Q, D_0, and μ

The Hamiltonian parameters used to get the numerical results reported in this paper consist of two sets that are summarized in Table I. In set I, $U=3t$, $V=t$, $t'=-0.25t$, and $t''=t'''=0$. In set II, $U=2.8t$, $V=0.85t$, $t'=-0.16t$, $t''=0.01t$, and $t'''=-0.05t$. The unit of energy is $t=1$ in both cases. Note that set I was used in Ref. 1 to study several of the ground-state properties of HTSC's within RAFT. Set II was used in Ref. 5 in the investigation of the effect of the PG on the charge-carrier density in HTSC's. To facilitate the discussion of finite temperature results, Q, D_0, and μ are shown again in Fig. 1 as a function of doping p at zero temperature for both parameters sets I and II. In both cases, as p increases Q decreases and vanishes at a critical value p_{QCP} (≈ 0.224 for set I and ≈ 0.161 for set II; see Table II), which has been interpreted as a quantum critical point.[1] D_0 on the other hand goes from being zero near half filling to a maximum value at p_{QCP}, then decreases for $p>p_{QCP}$ and vanishes in the heavily overdoped regime. Concerning the chemical potential μ, its p dependence shows a sudden change in the slope at p_{QCP}. The slope is smaller for $p<p_{QCP}$ than for $p>p_{QCP}$. Set II for this matter is more appropriate for the description of $La_{2-x}Sr_xCuO_4$ where the chemical potential has been reported to be practically flat

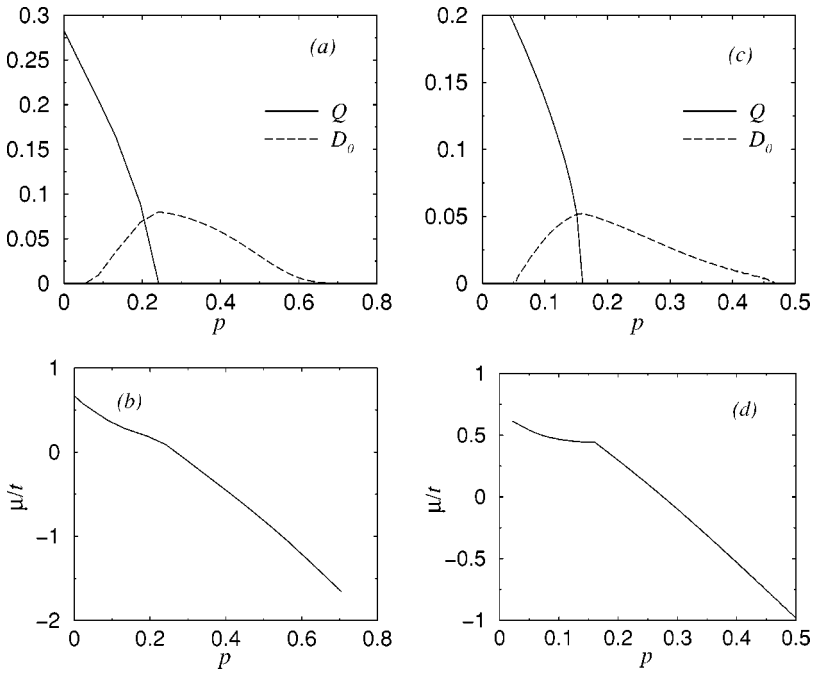

FIG. 1. The ground-state ($T=0$) parameters Q, D_0, and the chemical potential μ are displayed vs doping p. In (a) and (b) set I of parameters is used. In (c) and (d) set II is used. For both sets, Q vanishes at a quantum critical point that depends on the Hamiltonian parameters.

TABLE II. This table summarizes several quantities of interest for HTSC's. For both sets t is fixed so as to realize $T_C^{max}=100$ K.

	Set I	Set II
t (K)	714.3	1250
p_o	0.244	0.169
p_{QCP}	0.224	0.161
T_C^{max}	$0.14t=100$ K	$0.08t=100$ K
$T^*(p_o)$	$0.145t=104$ K	$0.149t=186$ K
$E_d(p_o)$	$0.325t=232$ K	$0.177t=221$ K
$U_0(p_o)$	$0.0084t=6$ K	$0.0035t=4.4$ K

below optimal doping but rapidly shifting above it.[12] For $Bi_2Sr_2Ca_{1-x}R_xCu_2O_{8+y}$, with $R=$Pr or Er, the shift in μ has been reported to be more pronounced in the underdoped regime than for $La_{2-x}Sr_xCuO_4$.[13] Parameters set I seems more adequate in this case for a qualitative description of the shift in μ.

B. The temperature dependence of Q and D_0

Only the results for set I are displayed in Fig. 2 for several doping densities. Note that instead of D_0, $2E_d \equiv 8VD_0$ is plotted. E_d is the amplitude of the d-wave energy gap. From Figs. 2(a) and 2(b), we see that for doping levels near the half-filling point $p(T=0)=0$, Q behaves as in a second-order phase transition with only one order parameter, meaning that it monotonously increases as temperature decreases to zero. For $p>0.07$, D_0 becomes nonzero below T_C and as a consequence Q decreases with T for $T<T_C$. Similarly, T^* will from now on designate the temperature below which Q switches on as T decreases from the high-temperature region. For p in the neighborhood of p_{QCP} the competition from SC is so strong that Q is nonzero only for an interval of temperature roughly centered around T_C for set I, and is zero for smaller temperatures including $T=0$. The state with $Q=0$ displays a reentrance behavior at lower temperatures as illustrated in Fig. 2(f). The normal-state properties are therefore affected for $p\sim p_{QCP}$ even though Q vanishes at zero temperature. The DDW theory exhibits a similar reentrance behavior to the present one. In summary, Figs. 2(c) and 2(e) show that SC and RAF can coexist, and that both parameters Q and D_0 turn on at T_C and T^*, respectively, and stay nonzero for all smaller temperatures. The competition between SC and RAF is evident at finite temperature in Figs. 2(d)–2(f), for a depression in Q takes place as soon as D_0 becomes nonzero. My results for Q below T_C are not consistent with neutron and muon experiments which seem to indicate that the magnetic moments observed by Mook[14] are slightly enhanced when temperature crosses over T_C. This is also a problem that the DDW theory faces.[15] Note that the origin of these moments is not yet known. As for set II some results were shown in Ref. 5. The major difference between the results for set I and set II shows for the parameter Q near p_{QCP}. For set II, Q is nonzero for a T interval well above T_C for $p\sim p_{QCP}$.

C. The temperature dependence of doping p

The results for p versus T in the case of set I are similar to those of set II, which were discussed in Ref. 5. Figure 2 displays the results for set I. In summary, I find that whereas p varies significantly with temperature when doping is initially small at $T=0$, it varies much less in the overdoped regime. A glance at Figs. 2(a–h) reveals that the PG parameter Q has the most noticeable effect on the temperature dependence of p than D_0 has. Except for the half-filled case where anyway the present theory has to be modified to include true long-range AF order,[16] the increase in Q as temperature decreases reduces p when $T>T_C$. In the mixed state with $T<T_C$ where both Q and D_0 are nonzero, p increases when Q decreases. Therefore, according to our results the general trend is that an increase in Q leads to a reduction of the level of doping on CuO_2 layers. In the overdoped regime where $Q=0$, the opening of the superconducting gap with amplitude $E_d=4VD_0$ has a minor effect on p. Note that the T derivative of p presents a discontinuity at T_C for all doping levels. Like for set II of parameters,[5] I can conclude that the state with $Q\neq 0$ reduces the number of charge carriers available for SC as temperature decreases. This is consistent with the idea of the PG reducing the density of states available for SC in the PG state. The idea that some spectral weight is lost at lower temperature in the PG state was implied by entropy data.[17]

D. The temperature dependence of the Hall coefficient

In Ref. 5 this issue was discussed for set II of parameters. Here I will show that the main T dependence features are also seen in the case of set I. The temperature dependence of p reported here seems also less unusual when I reconsider the strong temperature dependence of the Hall coefficient R_H.[6–8] The electron occupation probability $n(\mathbf{k})$ within RAFT revealed the existence of pockets reminiscent of the hole pockets in doped Mott insulators in the underdoped regime.[1] If I assume that the density of charge carriers is given solely by the density of holes p in this regime, then the Hall coefficient per unit volume V_0 and number of copper atoms N in volume V_0 will be roughly given by $R_H|e|/NV_0=1/p$, where e is the electron charge. Therefore, the temperature dependence of p can be compared to the experimental Hall density $n_H=NV_0/|e|R_H$. Ando and co-workers[18,19] measured the Hall coefficient for the cuprate $Bi_2Sr_{2-x}La_xCuO_{6+\delta}$, and found that R_H/NV_0 displays a significant temperature dependence. Note that for $La_{2-x}Sr_xCuO_4$, R_H showed strong deviations from the simple $1/p$ law (with a T independent p) in the doping region where SC is present, and that R_H changes sign for $x>0.15$.[8] The $1/p$ behavior is well observed in the light doping limit $p<0.05$. In addition, the Hall carrier density n_H reported by Suzuki[7] interestingly show a minimum at a temperature $T\sim 10$–80 K in agreement with the presence of a minimum in my results for p versus T. Note that the temperature derivative of p shows a discontinuity at T_C in my results, and that the minimum in p occurs exactly at T_C. Interestingly, the data of Chaudhari *et al.*[6] for n_H of epitaxial films of $YBa_2CuO_{7-\delta}$ show a minimum at exactly T_C and a linear

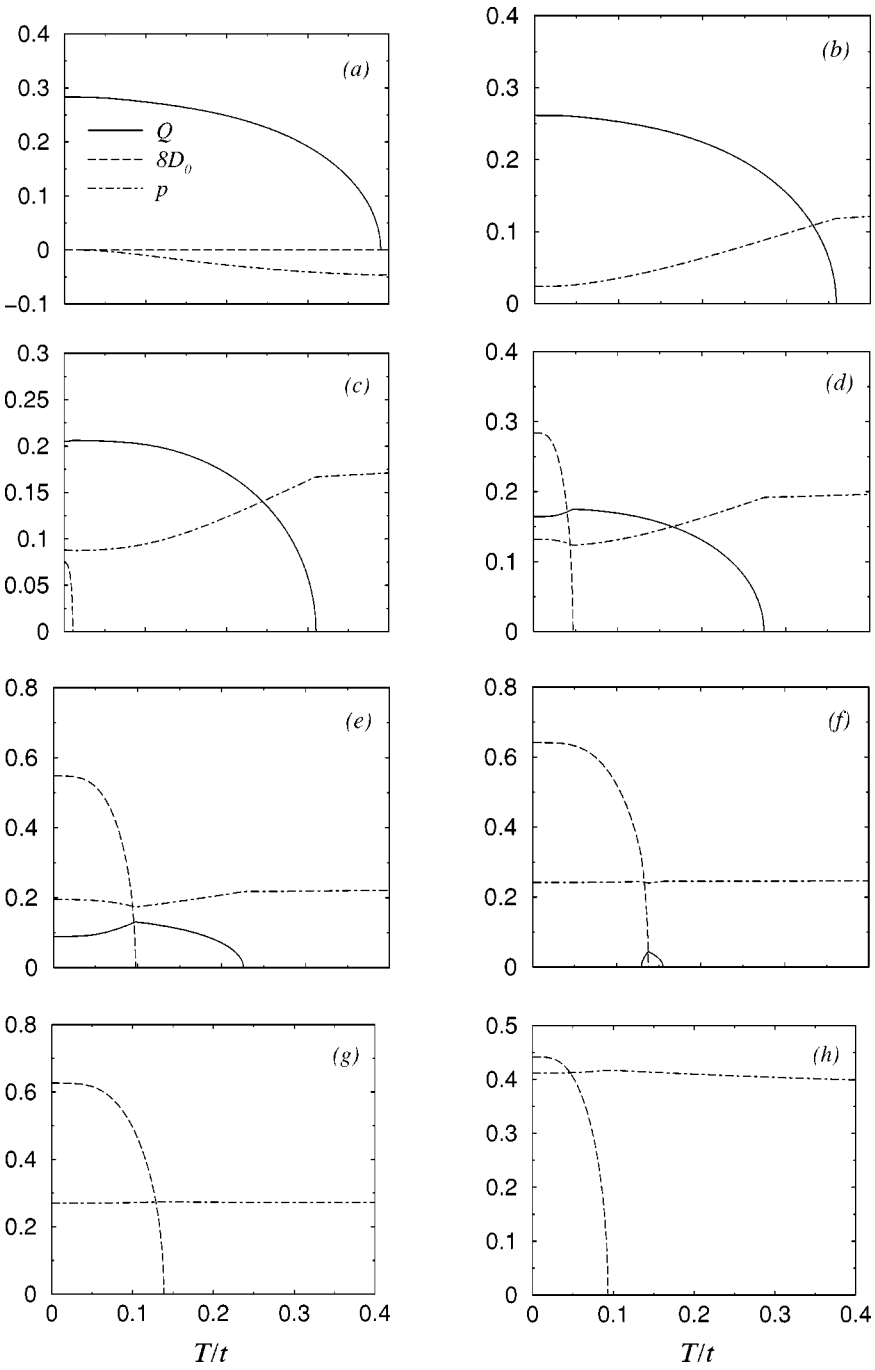

FIG. 2. The parameters Q, D_0, and the doping density p are displayed vs temperature for Hamiltonian parameters of set I.

dependence on T above T_C, which is in very good agreement with the one displayed by p versus T in Figs. 2(d) and 2(e). So, the proposal of a T dependent hole density seems to be very appropriate for the explanation of the strong and linear T dependence of the Hall coefficient for a wide range of temperature.

I should now mention that the distinction between different doping regimes in my calculations is done using the values p takes at zero temperature. This is how I proceeded in order to calculate the phase diagrams in the following section. This procedure is different from the one of experimentalists who use the room-temperature values for R_H to deduce the charge-carrier density on the CuO_2 layers.

IV. THE DOPING DEPENDENCE OF T_C AND T^*

A. The phase diagram for parameters set I

The phase diagram for the PG and superconducting states calculated for set I of the Hamiltonian parameters is depicted in Fig. 3(a). T^* and T_C are displayed as a function of p. The PG temperature T^* decreases almost linearly with doping, but for p slightly smaller than p_{QCP} the decrease in T^* becomes much more pronounced, and T^* goes from being almost equal to T_C at p_{QCP} to zero discontinuously. Therefore, the PG parameter Q and temperature T^* do not scale in the same way as a function of doping since Q seems to vanish continuously at p_{QCP}; very close to p_{QCP}, Q is found to

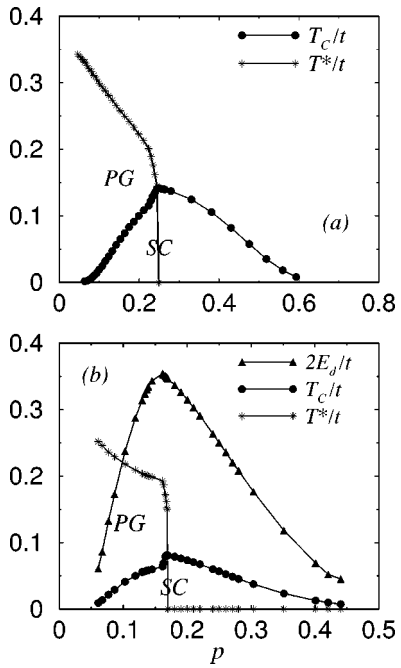

FIG. 3. The superconducting critical temperature T_C and the PG temperature T^* are plotted vs doping in the case of set I in (a) and set II in (b) for comparison. In (b) $2E_d$ is also reported vs doping. The solid line for T^* is only a guide to the eye. The symbols show the doping levels for which the calculation was carried out.

assume smaller values than D_0. Experimentally, the PG energy was reported to fall to zero linearly and continuously in p.[20] But in a recent paper, Naqib and co-workers[21] reported an experimental behavior with which my theoretical result is consistent. The maximum superconducting transition temperature T_C^{max} takes place at the optimal density p_o (Table II).

Figure 3(a) shows that $T^* \approx T_C^{max} \approx 0.14t$ at p_o, and stays always greater than T_C for smaller dopings. In a sense T^* merges into T_C at p_{QCP} because of the discontinuity in T^*, but in the competition scenario rather than the preformed pairs scenario. Note that although set I is not really adequate to fit yttrium barium copper oxide (YBCO) materials data because the lower and upper doping bounds of the superconducting dome do not match the experimental ones, I will use it for a qualitative description of these systems. To realize a maximum T_C of about $T_C^{max}=100$ K, t needs to be about 714 K, which yields a bandwidth of ≈ 7000 K, and a Fermi temperature very likely of the order of 1000 K in accord with Loram *et al.* conclusion.[9] However, the typical value T^* is believed to assume at zero doping is about 700 K or greater. This is at least seven times greater than T_C^{max}. In Fig. 3(a) the results for set I give a smaller ratio. It is for this reason that V has to be taken to be smaller than t. I will examine the phase diagram obtained using set II, which indeed gives a better value to this ratio, namely, $T^*(p=0)/T_C^{max} \approx 5$.

B. The phase diagram for parameters set II

The phase diagram shown in Fig. 3(b) for set II seems to agree well with the phase diagram of $La_{2-x}Sr_xCuO_4$ as far as the SC and PG phases are concerned. In this figure, T_C, T^*, and also $2E_d$ are displayed as a function of p. The superconducting dome takes place practically for $0.05 \leqslant p \leqslant 0.46$, and overall T_C and T^* behave similarly as in set I, but with the decrease of Q being less sharp away from p_{QCP}, and much sharper in the immediate vicinity of p_{QCP}. In comparison to the phase diagrams shown in Fig. 3, the one calculated within the DDW approach looks very different than the experimental one.[22] In the DDW approach, the DDW parameter vanishes for a hole density smaller than optimal doping. In my case, T^* vanishes very slightly above the optimal point. The latter behavior is the one that is more suitable for the description of HTSC's phase diagram.

TABLE III. Set II parameters used to model $La_{2-x}Sr_xCuO_4$ are shown. The question mark indicates that the experimental value of t is not yet precisely known and is model dependent. The experimental values are gathered from references as discussed in the text. p_{min} and p_{max} refer to the lower bound and upper bound of the superconducting dome as shown in Fig. 1, respectively. t, T_C^{max}, and E_d are given in kelvin.

	t	T_C^{max}	$E_d(p_o)$	p_{min}	p_{max}	p_o
Theory	500	40	87	0.05	0.46	0.169
Experiment	?	38	140	0.05	0.3	~ 0.15

For set II, now the value of T^* at p_o is approximately $0.15t$ which is as much as twice the optimal $T_C^{max} \approx 0.08t$. To realize $T_C^{max}=100$ K one needs $t=1250$ K. Table II presents a summary of experimental estimates for T_C, T^*, and E_d at p_o for both sets I and II. For $La_{2-x}Sr_xCuO_4$, the optimal $T_C^{max} \approx 40$ K yields $t=500$ K which still gives a bandwidth of the order of 1000 K. Table III summarizes the values of several quantities obtained by attempting to model $La_{2-x}Sr_xCuO_4$. The maximum superconducting energy-gap amplitude is $E_d=87$ K$=7.5$ meV. This is not in very good agreement with the experimental value of the gap ($\sim$10–15 meV) measured at optimal doping.[23,24] However, for the main purpose of this work this is not critical as I am concerned with getting a qualitative understanding of HTSC's using RAFT. For this reason the agreement can be seen to be rather satisfactory.

One may ask which one of the phase diagrams shown in Fig. 3 is suitable for HTSC's? Well, both may be. Recently, Naqib *et al.*[21] published a resistivity study of the material $Y_{1-x}Ca_xBa_2(Cu_{1-y}Zn_y)_3O_{7-\delta}$. For zero Zn and Ca doping, the phase diagram for set I seems more appropriate. With Zn and Ca doping, experimentally the optimal T_C diminishes but T^* is reported to stay practically the same at optimal doping. The phase diagrams for 20%Ca-1.5%Zn-Y123 and 20%Ca-3%Zn-Y123 look more like the one I get for set II of parameters. The sudden change in the slope of $T^*(p)$ near p_o seems also plausible in that experimental study.

C. The strong-coupling ratio $R=2E_d/k_BT_C$

For both sets of parameters, T_C displays a p dependence very similar to D_0, but with the strong-coupling ratio $R=2E_d/k_BT_C=8VD_0/k_BT_C$ not constant and strongly dop-

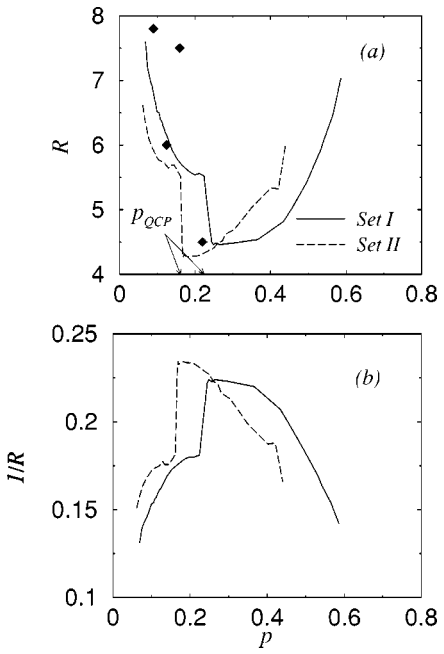

FIG. 4. (a) The ratio R is plotted vs p for parameters sets I and II. Diamonds are experimental data YBCO material taken from Ref. 27. (*b*) R^{-1} is shown vs p. For set I, R was already shown in Ref. 1, and is displayed again for comparison.

ing dependent. In BCS theory, R depends neither on the Fermi energy nor on the strength of the pairing coupling, and is therefore constant. Here the situation is different; I find that R depends on both doping and Hamiltonian parameters as shown for set I and set II in Fig. 4. The strong variation shown by R is remarkable because this has also been experimentally observed for $YBa_2Cu_3O_{7-\delta}$ and $Bi_2Sr_2CaCu_2O_{8+x}$ in the underdoped regime.[25,26] The overall variation of R with doping in the case of $YBa_2Cu_3O_{7-\delta}$ in the underdoped regime is well accounted for by my results as shown in Fig. 4(a). Ding *et al.*[27] discovered in an experiment on $Bi_2Sr_2CaCu_2O_{8+x}$ that the ratio $z_A E_d/k_B T_C$ is constant; z_A is the weight of the coherent quasiparticle peak at $(\pi,0)$ that appears below T_C in the spectral function. z_A showed a linear dependence on p giving rise to $R \sim p^{-1}$ in the underdoped regime. The latter dependence is also found to be satisfied within RAFT for $p < p_{QCP}$. For BCS superconductors, where the normal state is a Fermi liquid, z_A is constant and T_C is determined solely by one energy scale that is the superconducting gap. For HTSC's, RAFT proposes that this is not sufficient, and that doping plays a relevant role because T_C is determined by both the superconducting gap and doping level leading to $pR = p2E_d/k_B T_C$, a constant in the underdoped regime as illustrated in Fig. 4(b), where $1/R$ increases almost linearly with almost the same slope for both sets I and II. It remains to be seen if my prediction of R departing significantly form the optimal-point value in the overdoped regime can be corroborated by experiment.

Contrary to Ding *et al.*'s claim that E_d increases with decreasing p in the underdoped regime, I find that E_d decreases with p. As I already reported in Ref. 1, I believe that angle-resolved photoemission spectroscopy (ARPES) experiments are sensitive to the total single-particle gap which, in the underdoped regime, consists of the superconducting gap and pseudogap. There should be a distinction between the position of the coherent peak and its weight in ARPES spectra. My own interpretation of Ding *et al.*'s work is that all of the weight in the peak in the overdoped regime and most of it in the underdoped regime is a measure of superconductivity but the position does not necessarily reflect the superconducting gap in the underdoped region.

D. Degradation of superconductivity near optimal doping

Experimentally, a sudden degradation of SC is observed just below optimal doping in $La_{2-x}Sr_xCuO_4$.[8,28] This is signaled by a sudden decrease in T_C by almost 25% from the optimal T_C^{max}. Within RAFT, a degradation of SC is due to the sudden appearance of RAF below p_o at finite temperature, is more pronounced for set II than set I, and takes place slightly below optimal doping in excellent agreement with experiment. Note that T_C does not show a minimum contrary to what the midpoint determination of T_C for $La_{2-x}Sr_xCuO_4$ suggested.[29] For set II with $t = 500$ K, the fall in T_C is approximately $0.02t = 10$ K which is significant, and comparable to the decrease reported by Takagi *et al.*[8] Also, a sudden but less pronounced decrease of T_C is observed in T_C for $YBa_2Cu_3O_{6+x}$ below optimal doping.[9] Set I seems in this case more applicable. It is remarkable that the opening of the PG as a consequence of RAF not only steals away spectral weight available for SC and creates the optimal point in the vicinity of the QCP, but causes this sudden decrease in T_C as well. What is most remarkable above all is that RAFT is able to account for all these fine features and explain them in a simple and consistent way.

V. THE SPECIFIC-HEAT RESULTS

Within RAFT, the electronic specific-heat C_{el} is found by using the usual formula $C_{el} = T dS_{el}/dT$, which yields

$$C_{el}(T) = \frac{k_B}{4N} \sum_{\mathbf{k}} \sum_{\nu=1}^{2} \frac{\beta^2 \left[E_\nu^2(\mathbf{k}) - \frac{T}{2} \partial E_\nu^2(\mathbf{k})/\partial T \right]}{\cosh^2[\beta E_\nu(\mathbf{k})/2]}, \quad (9)$$

where S_{el} is the electronic entropy. The latter is given by

$$S_{el}(T) = -\frac{k_B}{N} \sum_{\mathbf{k}} \sum_{\nu=1}^{2} \{f[E_\nu(\mathbf{k})] \ln\{f[E_\nu(\mathbf{k})]\} + \{1 - f[E_\nu(\mathbf{k})]\} \ln\{1 - f[E_\nu(\mathbf{k})]\}\}, \quad (10)$$

with $f(x) = (1 + e^{\beta x})^{-1}$ being the Fermi-Dirac factor. In the numerical calculation $k_B = 1$. Next, I will start discussing the behavior of the specific-heat coefficient $\gamma = C_{el}(T)/T$.

A. The specific-heat coefficient $\gamma(T)$

1. Set I

The temperature dependence of $\gamma(T)$ is shown in Fig. 5 in the case of set I and for several doping levels. By examining Fig. 3(a), we find that deep in the underdoped regime T^* is

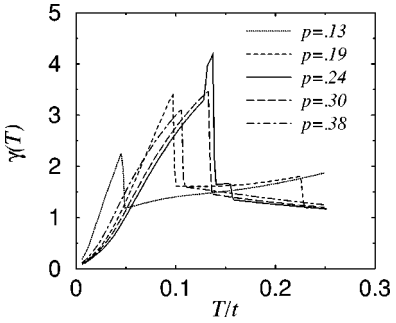

FIG. 5. The specific-heat coefficient $\gamma(T)=C_{el}/T$ is displayed for several doping levels in the case of set I of parameters.

much greater than T_C, and thus cannot manifest itself even for temperature of the order of $0.2t$ (about 200 K for $t \sim 1000$ K). For p in the vicinity of p_{QCP}, the anomaly in $\gamma(T)$ due to T^* is significantly smaller than the one due to T_C. The reason for the absence of the T^* anomaly so far in γ, experimentally, is perhaps due to the fact that the anomaly jump, being smaller, goes unnoticed in comparison to the superconducting jump in $\gamma(T)$. In addition, for $p \sim p_{QCP}$, it may easily be washed out by the superconducting one or the superconducting fluctuations because of the peculiar behavior of Q as shown in Fig. 2(f). In this case, the PG anomaly seems to enhance the SC jump and looks more like a step rather than a λ-type jump for $p=0.24$ and $p=0.19$. In summary, set I suggests that experimentally it is difficult to resolve the T^* jump because the T_C anomaly is greater and perhaps because of the transition fluctuations (in experiment) that round up these anomalies. In comparison, the specific-heat coefficient calculated within the DDW theory by Wu and Liu[15] shows a jump due to the DDW parameter, which is greater than the superconducting one in the underdoped regime. For this reason, my results seem more adequate for fitting experiment than DDW ones.

Once again, we notice that the parameters set I seems reasonable for fitting the data of the specific-heat of $Y_{0.8}Ca_{0.2}Ba_2Cu_3O_{7-\delta}$.[17] Indeed for this material, in the overdoped regime the normal state $\gamma(T)$ depends weakly on temperature like in my results, whereas in the underdoped regime a significant decrease of $\gamma(T)$ with T is observed above T_C. There is an important difference however between the overall temperature dependence of my theoretical results and the experimental data in the underdoped regime because the peak in $\gamma(T)$ due to SC stays always below the largest peak that takes place at optimal doping in experiment contrary to my findings. Roughly, $\gamma(T)$ versus T reflects the energy dependence of the density of states (DOS). In the underdoped region, I thus find that the DOS is depressed as temperature decreases when $T>T_C$ in agreement with the signature of the PG.[17]

2. Set II

Figure 6 shows $\gamma(T)$ for parameters set II. Now, the anomaly due to T^* in γ can be seen only for temperatures $T>0.15t$ even though $T_C^{max} \approx 0.08t$. Figure 6(a) shows again that this anomaly is much smaller than the T_C anomaly, and

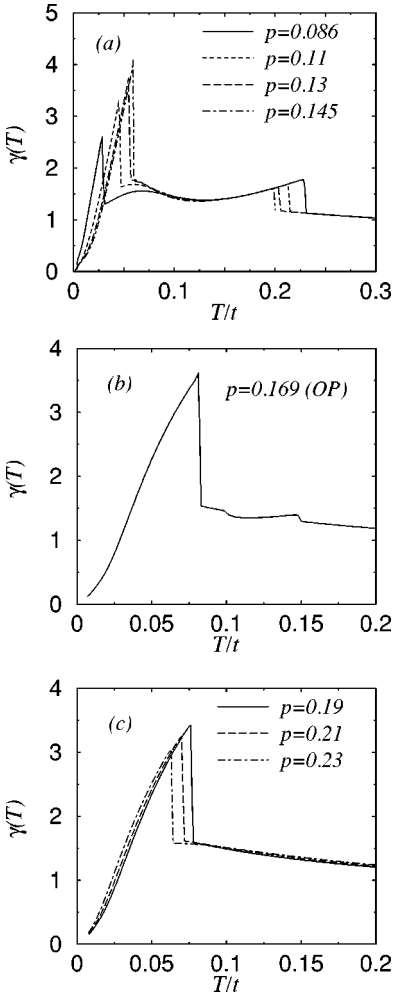

FIG. 6. The coefficient $\gamma(T)$ is plotted vs temperature in the underdoped regime (a), at optimal doping (b), and in the overdoped regime (c) for several doping levels and for parameters set II.

that it becomes less pronounced as doping approaches the optimal point. For the temperatures of interest (usually the experimental specific-heat is measured for temperatures up to about 200 K or so) it is likely that T^* is barely within the range of these temperatures. For $t=1250$ K, for example, $T^*=186$ K (Table II). Set II of parameters seems more appropriate to model $La_{2-x}Sr_xCuO_4$. Indeed the behavior shown by $\gamma(T)$ in Fig. 6 resembles the experimental one reported by Loram *et al.*[17] where $\gamma(T)$ shows a broad maximum above T_C in the underdoped regime, and a substantial increase above the T_C anomaly in the overdoped regime. The PG signature consisting of $\gamma(T)$ decreasing in the underdoped region is in this case clearly seen for $p=0.086$ and 0.11. Note that the doping and temperature dependence of $\gamma(T)$ for set II differs from that of set I because of the broad maximum in $\gamma(T)$ for $T_C<T<T^*$. Concerning the signature of the T^* anomaly, it is interesting enough to note that the data of the $La_{2-x}Sr_xCuO_4$ material show what could be that signature. In Fig. 5 of Ref. 17, a hump can be seen in $\gamma(T)$ at a temperature $T \approx 200$–250 K that is about five times greater than $T_C^{max} \approx 40$ K. The signature for the T^* anomaly I get here occurs at $T \sim 3T_C^{max}$. It would be very interesting

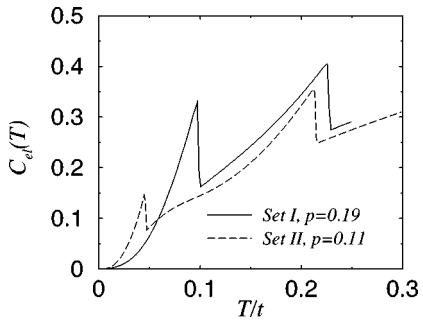

FIG. 7. The specific-heat $C_{el}(T)$ is displayed as a function of temperature for $p=0.19$ and $p=0.11$ for sets I and II, respectively.

to revisit the experimental data and check this claim by carefully measuring γ well above T_C, and following the precise doping dependence of those humps. In the overdoped regime, γ increases as T decreases in agreement also with experimental observation for $La_{2-x}Sr_xCuO_4$. At the optimal point in Fig. 6(b), two humps characterize $\gamma(T)$ above T_C due to the switching on and off of Q which takes place at $T\approx 0.15t$ and $T\approx 0.1t$, respectively.

So far I analyzed the specific-heat coefficient. However, it is interesting to examine the specific-heat and its anomaly at T^*. For both parameters sets, the T^* anomaly is more spectacular in the specific-heat C_{el} itself than in $\gamma(T)=C_{el}(T)/T$. Indeed, the T^* anomaly in γ is significantly enhanced when it is multiplied by T^*. Figure 7 illustrates this behavior for two doping levels in the underdoped regime for set I and set II. The specific-heat jump at T^* is at least as pronounced as at T_C for both sets. To the best of my knowledge, it was always the experimental data of γ not C_{el} that have been reported; perhaps because γ reflects the energy dependence of the DOS. The peak in C_{el} at T^*, which is broader than at T_C, does not signal a phase transition from a disordered state to an ordered state in the conventional way. For $T<T^*$, the PG state neither breaks rotational symmetry nor has long-range order.

B. The entropy $S_{el}(T)$

1. Set I

I calculated the entropy per site $S_{el}(T)$ for several doping levels and reported it in Fig. 8 as a function of temperature

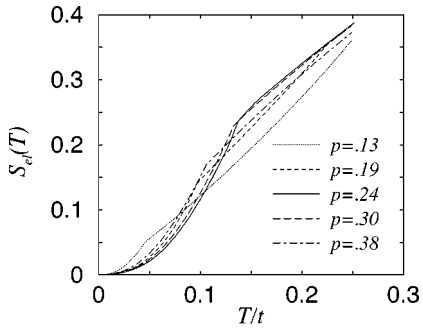

FIG. 8. The entropy $S_{el}(T)/k_B$ is displayed as a function of temperature for several doping levels in the case of parameters set I.

for parameters set I. My results compare well with the experimental results of Ref. 9 not only for the general trends of the doping dependence, but also for the magnitude of S_{el}. For $p=0.24$, for example, which is close to the optimal doping point, $S_{el}(T_C)\approx 0.24$ is comparable to the experimental value 0.22 for $YBa_2Cu_3O_{6+x}$ with $x=0.97$. I find that for $p=0.13$, $S_{el}(T_C)\approx 0.05$. The latter value would correspond to $x=0.57$ in $YBa_2Cu_3O_{6+x}$ where $S_{el}(T_C)=0.06$. For $p=0.13$ and 0.19, $S_{el}(T)\sim T^n$, with $n>1$, in the normal state. But for $p=0.24$, 0.3, and 0.38 in the overdoped regime $S_{el}\sim T^n$, with now $n<1$. This implies a regime change for p nearby p_o. It is possible that in the normal state $S_{el}\sim T$ in the immediate vicinity of optimal doping, as found in experiment. Loram and co-workers[9] concluded for no evidence in their entropy data for independent excitations with different statistics. As mentioned earlier, they also said that the simplest interpretations of S_{el} could be done in terms of fermionic carriers with very low Fermi temperature ~ 1000 K. RAFT is consistent with this interpretation. Note that the superconducting transition manifests itself clearly as a kink in $S_{el}(T)$ at T_C, but the PG kink is difficult to see at T^*. In Fig. 8, in the underdoped regime $S_{el}(T)$ shows some entropy loss for $T<T^*$ which is due to the loss of spectral weight consistently with the decrease of γ below T^*. Experimentally, entropy loss is also seen and is permanent,[17] meaning that the entropy lost at low T is not regained at sufficiently high T. Consequently the opening of the PG does not conserve the DOS.

2. Set II

$S_{el}(T)$ is displayed in Fig. 9 in the case of set II. A similar discussion as for set I can be made and applied rather to $La_{2-x}Sr_xCuO_4$. Here, in the overdoped regime, $S_{el}\sim T^n$ with n very slightly smaller than 1. At optimal doping S_{el} is pretty linear in T, and in the underdoped regime, the curvature of S_{el} changes from positive to negative with T decreasing while $T_C<T<T^*$.

VI. THE DOPING DEPENDENCE OF SUPERFLUIDITY

I have calculated the doping dependence of the jump in γ at T_C, $\Delta\gamma_C=\gamma(T_C^-)-\gamma(T_C^+)$, and reported it in Fig. 10 for both sets I and II. $\gamma(T_C^+)$ and $\gamma(T_C^-)$ designate the values γ assumes on the normal state and superconducting state sides of T_C, respectively. Except for the sharp peak at p_{QCP}, $\Delta\gamma_C$ shows a behavior similar to the experimental one in the underdoped regime as reported by Tallon and Loram[20] for Bi based materials. $\Delta\gamma_C$ increases with doping in the underdoped regime, and reaches a maximum at p_{QCP}, then drops in the overdoped regime. Consistently with Tallon and Loram's proposal, the fact that (experimentally) $\Delta\gamma_C$ decreases sharply with underdoping is a proof that the PG cannot be a consequence of SC phase fluctuations. This is a behavior one would expect from a competition scenario where the PG phenomenon is stealing away spectral weight otherwise available for SC.

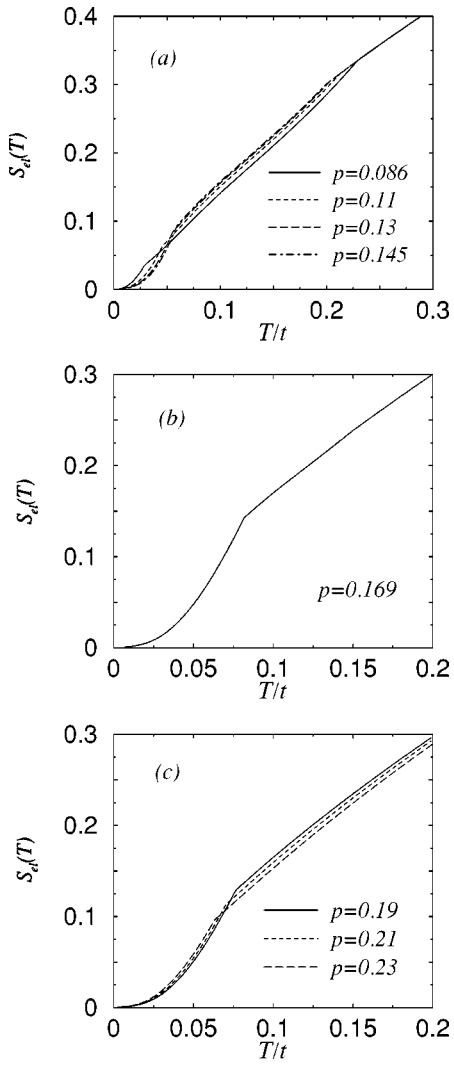

FIG. 9. The entropy $S_{el}(T)/k_B$ for parameters set II is displayed as a function of temperature for several doping levels in the underdoped regime (a), at optimal doping (b), and in the overdoped regime (c).

Figure 11 shows the doping dependence of the entropy at T_C, $S_{el}(T_C)$. This compares qualitatively very well with $Y_{0.8}Ca_{0.2}Ba_2Cu_3O_{7-\delta}$ data[20] where $S_{el}(T_C)$ increases linearly with p in the underdoped region, reaches a maximum near optimal doping, and decreases in the overdoped regime.

On the other hand, I calculated the doping dependence of the superconducting condensation energy U_0 which is the change in free energy in transforming from the normal state to the superconducting one at zero temperature. Figure 12 shows the doping dependence of U_0 for sets I and II. This doping dependence is similar in many aspects to the experimental one obtained by integrating entropy data by Loram *et al.*[17] for $Y_{0.8}Ca_{0.2}Ba_2Cu_3O_{7-\delta}$ systems. In the overdoped regime, U_0 decreases for p greater than the optimal point consistently with the decrease in T_C. Below the optimal point, U_0 decreases with underdoping again consistently with the experimental observation. A maximum characterizes U_0 at p_{QCP} like in experimental data near optimal doping. Again, this behavior was proposed not to be consistent with

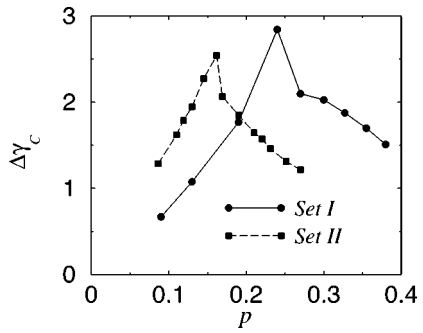

FIG. 10. $\Delta\gamma_C = \gamma(T_C^-) - \gamma(T_C^+)$ is plotted as a function of doping. Solid circles and squares correspond, respectively, to parameters sets I and II.

preformed pairs scenario. It strongly suggests a scenario with two competing order parameters in the underdoped regime. Because the PG parameter Q persists to temperatures smaller than T_C, which means that RAF and SC coexist and compete against each other for $T<T_C$, U_0 is reduced leading to the weakening of the superconducting condensate in the underdoped regime.

$\Delta\gamma_C$ and U_0 show a remarkable resemblance with the measured superfluid density ρ_s and the superconducting peak ratio (SPR).[30,31] SPR measures the relative intensity of the superconducting peak in ARPES at $(\pi,0)$ and the total spectrum intensity.[31] SPR and ρ_s were found to scale with p but not with $1-p$ in the underdoped regime. This is in agreement with my results for $\Delta\gamma_C$ and U in my competing orders scenario nearby the quantum critical point p_{QCP}. As Feng *et al.*[31] concluded, this behavior is not reminiscent of a BCS description based on the Fermi-liquid theory of the superconducting state, but rather agrees with theories that are based on doped Mott insulator like in RAFT. This justifies my assumption for the nature of the charge carriers being holes that was proposed for R_H earlier on.[5] Panagopoulos and co-workers[32] pointed out that $S/T(T_C)$ is a measure of the energy-dependent DOS averaged over $\pm 2k_BT$ around the Fermi energy. The superfluid density ρ_s is related to the available DOS. So the strong suppression of the DOS, implied by the decrease of $S(T_C)$, with underdoping signals the strong decrease of ρ_s.

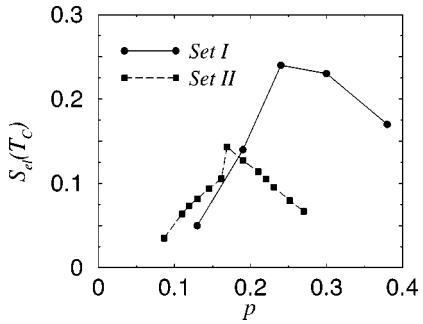

FIG. 11. $S_{el}(T_c)$ is plotted vs doping p. Solid circles and squares correspond, respectively, to parameters sets I and II.

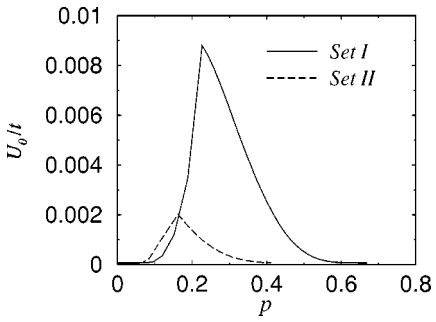

FIG. 12. The condensation energy U_0 is plotted vs doping p. The full line and dashed line correspond to set I and set II parameters sets. U_0 shows a sharp peak at p_{QCP}.

VII. SUMMARY AND CONCLUSIONS

In this work, I tested the applicability of the rotating antiferromagnetism theory (RAFT) of high-temperature superconductors by calculating several thermodynamic quantities. I used my earlier proposal of the CuO_2 layers behaving as open systems in contact with an electron reservoir,[5] and calculated several thermodynamic functions. The charge-carrier density becomes temperature dependent, meaning that when temperature varies the number of holes (electrons) varies too. This is very interesting in view of the permanent loss of spectral weight observed in specific-heat data, and also in view of the strong temperature dependence shown by the Hall coefficient. This indeed explains the linear temperature dependence observed in the Hall coefficient experimentally.

Although the order parameter associated with the pseudogap energy shows a behavior slightly different from the experimentally suggested one for $T<T_C$, overall very good agreement with experiment is achieved for the doping and temperature dependence of the specific-heat coefficient and entropy, and for the doping dependence of the condensation energy. By varying the Hamiltonian parameters I was able to propose two different scenarios for the doping dependence of the pseudogap temperature T^*. Figure 3 summarizes this finding for two Hamiltonian parameters sets I and II. In both scenarios, the jump in the specific-heat coefficient $\Delta\gamma(T^*)$ at the RAF transition temperature T^* looks more like a step than a λ, and is found to be much smaller than the jump at T_C. Whereas in scenario II (with parameters set II), T^* stays much higher than T_C even near optimal doping, in scenario I (with set I) T^* becomes equal to T_C at optimal doping. Very interestingly, changing the Hamiltonian parameters from set I to set II seems to simulate the effect of doping with Ca and Zn Y123 materials.[21] Also, I proposed that the reason for the absence of the signature of the pseudogap anomaly in $\gamma(T)$ in experiment can be explained by either the fact that it is much smaller than the one of T_C (for set I) or by the fact that it occurs at temperatures much higher than T_C^{max} and that it is much smaller than the one of T_C (for set II). In addition, I found that there exists a sudden depression in T_C right below optimal doping in agreement with experimental data for $La_{2-x}Sr_xCuO_4$, for example. This depression is more significant for parameters set II than set I. My conclusion regarding the doping dependence of superfluidity is in good agreement with published experimental results by Feng and co-workers. It shows a sharp peak nearby the quantum critical point, and scales with doping p rather than with electron density $1-p$ in the underdoped regime.

Overall, the most important aspect of the present theory is its universality in the sense that it is possibly applicable to different high-T_C materials, and to different physical phenomena taking place in these materials. A work using RAFT addressing the transport properties, which seems to confirm this universality, is in progress, and will be reported shortly.

ACKNOWLEDGMENTS

The author thanks K. Hewitt and H. J. Kreuzer for their comments and acknowledges financial support from NSERC of Canada.

[1] M. Azzouz, Phys. Rev. B **67**, 134510 (2003).
[2] T. Timusk and B. Statt, Rep. Prog. Phys. **62**, 61 (1999).
[3] J.G. Bednorz and K.A. Müller, Z. Phys. **64**, 189 (1986).
[4] S. Chakravarty, R.B. Laughlin, D.K. Morr, and C. Nayak, Phys. Rev. B **63**, 094503 (2001).
[5] M. Azzouz (unpublished).
[6] P. Chaudhari, R.T. Collins, P. Freitas, R.J. Gambino, J.R. Kirtley, R.H. Koch, R.B. Laibowitz, F.K. LeGoues, T.R. McGuire, T. Penney, Z. Schlesinger, A.P. Segmüller, S. Foner, and E.J. McNiff, Jr., Phys. Rev. B **36**, 8903 (1987).
[7] M. Suzuki, Phys. Rev. B **39**, 2312 (1989).
[8] H. Takagi, T. Ido, S. Ishibashi, M. Uota, and S. Uchida, Phys. Rev. B **40**, 2254 (1989).
[9] J.W. Loram, K.A. Mirza, J.R. Cooper, and W.Y. Liang, Phys. Rev. Lett. **71**, 1740 (1993).
[10] M. Azzouz, Phys. Rev. B **62**, 710 (2000).
[11] One of the earliest works that used the extendend Hubbard model for HTSC's is done by R. Micnas, J. Ranninger, S. Robaszkiewicz, and S. Tabor, Phys. Rev. B **37**, 9410 (1988).
[12] A. Ino, T. Mizokawa, A. Fujimori, K. Tamasaku, H. Eisaki, S. Uchida, T. Kimura, T. Sasagawa, and K. Kishio, Phys. Rev. Lett. **79**, 2101 (1997).
[13] N. Harima, A. Fujimori, T. Sugaya, and I. Terasaki, Phys. Rev. B **67**, 172501 (2003).
[14] H.A. Mook, P. Dai, and F. Dogan, Phys. Rev. B **64**, 012502 (2001).
[15] C. Wu and W.V. Liu, Phys. Rev. B **66**, 020511 (2002).
[16] It is possible to include long-range order for p near half filling.
[17] J.W. Loram, K.A. Mirza, J.R. Cooper, and J.L. Tallon, J. Phys. Chem. Solids **59**, 2091 (1998).
[18] Y. Ando, T. Murayama, and S. Ono, Physica C **341-348**, 1913 (2000).
[19] Y. Ando, Y. Hanaki, S. Ono, T. Murayama, K. Segawa, N. Miyamoto, and S. Komiya, Phys. Rev. B **61**, R14 956 (2000).
[20] J.L. Tallon and J.W. Loram, Physica C **349**, 53 (2001).
[21] S.H. Naqib, J.R. Cooper, J.L. Tallon, and C. Panagopoulos,

Physica C **387**, 365 (2003).
[22] J.-X. Zhu, W. Kim, C.S. Ting, and J.P. Carbotte, Phys. Rev. Lett. **87**, 197001 (2001).
[23] X.K. Chen, J.C. Irwin, H.J. Trodahl, T. Kimura, and K. Kishio, Phys. Rev. Lett. **73**, 3290 (1994).
[24] A. Ino, C. Kim, T. Mizokawa, Z.-X. Shen, A. Fujimori, M. Takaba, K. Tamasaku, H. Eisaki, and S. Uchida, J. Phys. Soc. Jpn. **68**, 1496 (1999).
[25] N.-C. Yeh C.-T. Chen, G. Hammerl, J. Mannhart, A. Schmehl, C.W. Schneider, R.R. Schulz, S. Tajima, K. Yoshida, D. Garrigus, and M. Strasik, Phys. Rev. Lett. **87**, 087003 (2001).
[26] N. Miyakawa, P. Guptasarma, J.F. Zasadzinski, D.G. Hinks, and K.E. Gray, Phys. Rev. Lett. **80**, 157 (1998).
[27] H. Ding, J.R. Engelbrecht, Z. Wang, J.C. Campuzano, S.-C. Wang, H.-B. Yang, R. Rogan, T. Takahashi, K. Kadowaki, and D.G. Hinks, Phys. Rev. Lett. **87**, 227001 (2001).
[28] T. Nagano, Y. Tomioka, Y. Nakayama, K. Kishio, and K. Kitazawa, Phys. Rev. B **48**, 9689 (1993).
[29] See K. Yamada, C.H. Lee, K. Kurahashi, J. Wada, S. Wakimoto, S. Ueki, H. Kimura, Y. Endoh, S. Hosoya, G. Shirane, R.J. Birgeneau, M. Greven, M.A. Kastner, and Y.J. Kim, Phys. Rev. B **57**, 6165 (1998) for a survey.
[30] A. Damascelli, D.H. Lu, and Z.-X. Shen, J. Electron Spectrosc. Relat. Phenom. **117-118**, 165 (2001), and references therein.
[31] D.L. Feng, D.H. Lu, K.M. Shen, C. Kim, H. Eisaki, A. Damascelli, R. Yoshizaki, J.-i. Shimoyama, K. Kishio, G.D. Gu, S. Oh, A. Andrus, J. O'Donnell, J.N. Ekstein, and Z.-X. Shen, Science **289**, 277 (2000).
[32] C. Panagopoulos, B.D. Rainford, J.R. Cooper, W. Lo, J.L. Tallon, J.W. Loram, J. Betouras, Y.S. Wang, and C.W. Chu, Phys. Rev. B **60**, 14 617 (1999).